

Trajectory Tracking Control of Dual-PAM Soft Actuator with Hysteresis Compensator

Junyi Shen¹, Tetsuro Miyazaki¹, Shingo Ohno², Maina Sogabe¹, and Kenji Kawashima¹

Abstract—Soft robotics is an emergent and swiftly evolving field. Pneumatic actuators are suitable for driving soft robots because of their superior performance. However, their control is not easy due to their hysteresis characteristics. In response to these challenges, we propose an adaptive control method to compensate hysteresis of a soft actuator. Employing a novel dual pneumatic artificial muscle (PAM) bending actuator, the innovative control strategy abates hysteresis effects by dynamically modulating gains within a traditional PID controller corresponding with the predicted motion of the reference trajectory. Through comparative experimental evaluation, we found that the new control method outperforms its conventional counterparts regarding tracking accuracy and response speed. Our work reveals a new direction for advancing control in soft actuators.

I. INTRODUCTION

Soft robotics, a field driven by the utilization of flexible, lightweight structures with infinite degrees of freedom, offers a safe and natural human-machine-interface during collisions or impacts [1]. It has seen exponential growth due to the development of soft actuators constructed from resilient materials, such as silicone rubber and shape memory alloys [2], [3]. These materials' innate flexibility provides the crucial adaptability for diverse applications, ranging from medical devices and rehabilitation aids to delicate industrial tasks [4]–[6].

Soft robotic motion depends on various deformations of flexible actuators, with pneumatic actuation playing a significant role. Pneumatic artificial muscles (PAMs), for instance, based on the McKibben artificial muscle design, replicate biological muscle movements and are praised for their cost-effectiveness and high force-to-weight ratio [7]. Pneumatic bending actuators, typified by multiple miniature compartments, further advance this field, enabling intricate movements and interactions [8]–[10].

While soft actuators' versatility benefits soft robotics, it also introduces challenges, particularly in tasks requiring precision [11]. A significant hurdle is hysteresis management — a nonlinearity resulting in delayed actuator response to control signal changes, which presents a challenge to real-time and precise control [12]. This issue is especially relevant to

pneumatic actuation due to its compressible nature, limiting the application range of pneumatic soft robots [8].

To mitigate hysteresis, two strategies have been widely adopted in contemporary research: model-based control algorithms and feedforward hysteresis compensation [13]. While model-based approaches view hysteresis as an unmodeled dynamic or disturbance to be alleviated through advanced nonlinear algorithms [14], other researchers employ modeling and compensation techniques using various play operators [15]. However, such strategies often encounter issues, such as the dependence on accurate linear approximation and the potential instability of the system, particularly with single-loop hysteresis models and play operator-based models [16]–[18]. Moreover, most existing models overlook the hysteresis loop deformation due to factors such as temperature changes and rubber creep. Therefore, considering the inherent complexities coupled with possible unreliabilities of these approaches and the high degrees of freedom in certain actuators, a more flexible control scheme is imperative [1], [10].

In this study, we achieved precise trajectory tracking by a novel dual-PAM bending actuator. Two PAMs are arranged antagonistically in this actuator to guarantee its rapid reaction towards changes in the desired position. This parallel configuration combines the advantages of compact structure found in antagonistic mechanisms with the adjustable rigidity and high power-to-volume ratio offered by PAMs [19]. Unlike conventional parallel manipulators, where motion control can be modeled and decomposed into the length control of PAMs [18], [20], this dual-PAM actuator achieves bending actuation through the continuum deformation of both PAMs and the elastic metal plate. Due to this unique mechanism, the motion of this actuator cannot be decomposed into linear movements of individual components, thus increasing the complexity for planning control using either model-based method or feedforward compensator. To address this challenge, we propose a simple yet effective scheme called *adaptforward* control. This approach dynamically adjusts the gains of a PID controller to mitigate the impact of hysteresis based on the predicted motion of the reference signal. To validate our control approach, we conducted comparative trajectory tracking experiments.

Ensuing sections provide an in-depth exposition of our methodology and findings. Section 2 details the design, operational principles, and hysteresis characteristics underpinning the dual-PAM soft actuator. Section 3 introduces the innovative *adaptforward* control method. Section 4 validates its efficacy through experimental evaluations, comparing the accuracy of bend angle tracking using the *adaptforward* strategy with conventional control methods. Lastly, Section

*This work has been submitted to the IEEE for possible publication. Copyright may be transferred without notice, after which this version may no longer be accessible.

¹Department of Information Physics and Computing, Graduate School of Information Science and Technology, The University of Tokyo, 7-3-1 Hongo, Bunkyo-Ku, Tokyo, Japan
kenji.kawashima@ipc.i.u-tokyo.ac.jp

²Innovative Project Planning and Promotion Department, Bridgestone Corporation, 3-1-1 Kyobashi, Chuo-Ku, Tokyo, Japan
shingo.oono@bridgestone.com

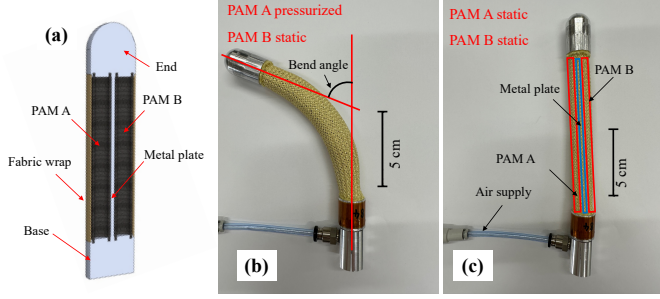


Fig. 1. Dual-PAM bending actuator: (a) basic configuration, (b) single PAM being pressurized, (c) both PAMs at static state.

5 draws a comprehensive conclusion.

II. ANTAGONISTIC DRIVEN TYPE PNEUMATIC BENDING ACTUATOR

A. Overall Configuration

Fig. 1 features the dual-PAM pneumatic bending actuator used in this work. Design of this actuator brings together an array of components: a metallic base, a pair of rubber chambers, a metallic end, a metal plate bridging the end and the base, and a fabric wrapping that laterally covers the actuator. This configuration enables both chambers to function as an independent PAM, even though they share one common fabric wrapping.

The dual-PAM actuator achieves controlled bending by leveraging the fundamental mechanism of PAMs. As illustrated in Fig. 1(b), when a single PAM is pressurized, it contracts and generates an axial tensile force toward the actuator end. By inducing a pressure differential between the two PAMs, an imbalance in generated force and displacement occurs on different sides of the metal plate, leading to its folding and driving the overall bending motion of the actuator. The antagonistically arranged PAMs ensure a rapid response of this actuator to the control signal and a two-directional bending ability that enhances the versatility of soft actuators to deal with unknown environment as depicted in Fig. 2. Additionally, this arrangement enables the realization of adjustable stiffness for the bending actuator by applying different pressurization combinations.

The bending angle of this actuator can be manipulated by adjusting the internal pressures within each PAM. When both PAMs are depressurized to zero, the actuator promptly returns to its initial straight state, as demonstrated in Fig. 1(c). This behavior is attributed to the elasticity of the metal plate, as the bending force applied does not exceed its elastic limit. Otherwise, irreversible deformation may occur, preventing the bending actuator from returning to its original shape.

Considering the symmetrical bending performance rooting from the design of this actuator, bending investigation is limited to one direction in this work for properly reducing the workload. However, the obtained results can be applied to bending in both directions under rigorous system design.

B. Hysteresis Characteristics of the Dual-PAM Actuator

1) *Overview of the Experimental Apparatus:* We obtained bending-pressure hysteresis loops of the dual-PAM bending actuator by experiments. Schematic of the experimental configuration is depicted in Fig. 3, encompassing components including the dual-PAM bending actuator, which is a prototype provided by Bridgestone, a pair of Festo MPYE-5-M5-010B flow control type servo valves, a BENDLABS-1AXIS bending angular sensor, two SMC PSE 540 A-R06 pressure sensors, and a computer system, within which a Contec AI-1616L-LPE analog board and a Contec AO-1608L-LPE analog board function respectively as the analog input board and the analog output board.

2) *Assessment of Bend-Pressure Hysteresis Loops:* Former research on hysteresis properties of PAMs uses position triangular pressure waveforms originating from completely depressurization atmospheric states [15], hence hysteresis properties during depressurization-pressurization state transition at various degrees of deformation are not revealed. To observe hysteresis properties existing in state transitions at low and high extents of deformation, we design the assessment of hysteresis properties to include measurements of hysteresis loops originating from two different initial states. In the first case, we establish the internal pressures of both PAMs at atmospheric levels and define the initial bending angle at zero. Subsequently, a positive triangular waveform with diminishing amplitude is employed to pressurize and depressurize PAM A, as illustrated in Fig. 4 (a). The second scenario establishes an initial pressure within PAM A at a high value of 420 kPa, then applies a negative triangular waveform with a decreasing amplitude, to alternately pressurize and depressurize PAM A, as illustrated in Fig. 4 (b). In the second measurement, the obtained minimum bending angle during the recording is set as the zero-bending point. Within (a) and (b), color distinctions represent different input pressure variations. Throughout experiments, the actuator's bending angle and internal pressure of PAM A are continuously recorded while the internal pressure of PAM B being maintained at a constant atmospheric value.

Obtained hysteresis loops corresponding to different changing directions and variations of internal pressures are illustrated in Fig. 5 (a) and (b), respectively. Arrows indicate the direction of loops. Line colors correspond to different pressure variations in Fig. 4. In (a) and (b), dead-zones and quasi dead-zones can be observed at the peak and bottom of each loop. Dead-zones emerging during the PAM's state transition from pressurization to depressurization are denoted in red, and those occurring during the transition from depressurization to pressurization are indicated in blue.

It can be discerned from Fig. 5 (a) that widths of those red zones displays an escalation with the increase of the bending angle and pressure values. Analogously, an inverse correlation can be identified in 5 (b) that widths of those blue patterns increases correspondingly with the decrease of the bending angle and internal pressure. The increase in widths of hysteresis dead-zones indicates an augment in the actuator's nonlinearity, which is consistent with [21] that the nonlinear

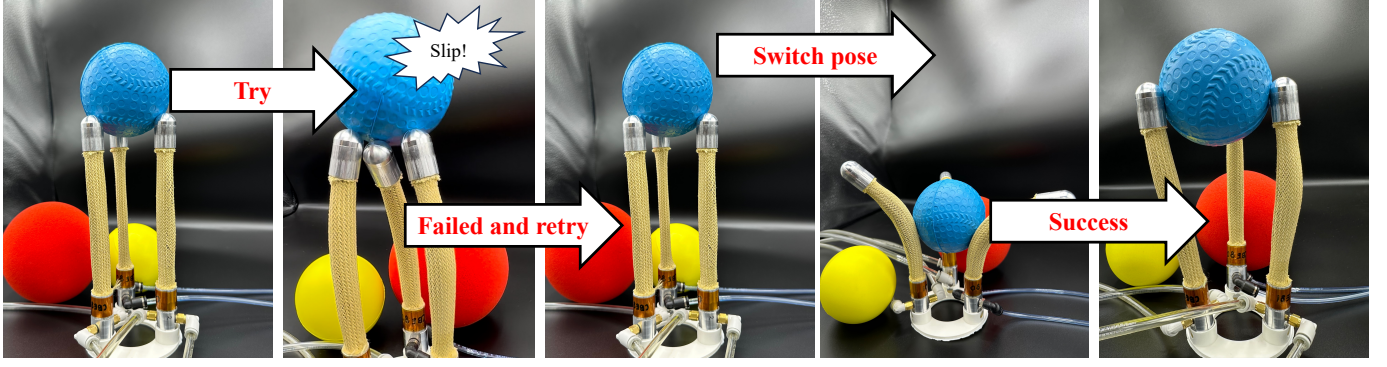


Fig. 2. Application of the dual-PAM actuator in soft grippers that are able to change poses for grasping object.

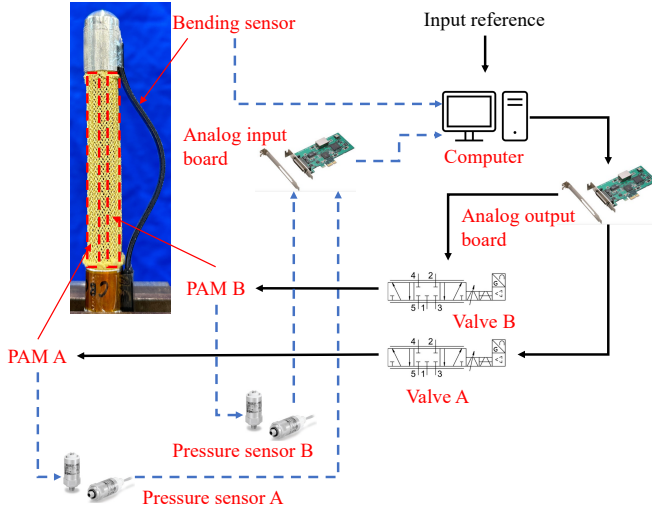


Fig. 3. Schematic of the experimental apparatus.

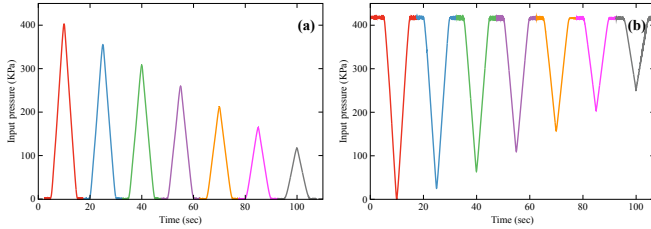


Fig. 4. Pressure variations in the pressurized PAM during experiments: (a) the first case from an atmospheric value, (2) the case instance from a preset high pressure.

property of PAMs becomes significant when the actuator is at an extremely high or low pressure value.

III. TRAJECTORY TRACKING CONTROL STRATEGY

While the integration of elastic metal components into the actuator design enhances the stiffness and response speed of soft actuator, it can potentially lead to fatigue and irreversible plastic deformation due to repetitive actuation in long-term use. These changes may alter the hysteresis property of the proposed bending actuator, affecting the reliability of the model-based control algorithms or feedforward compensation

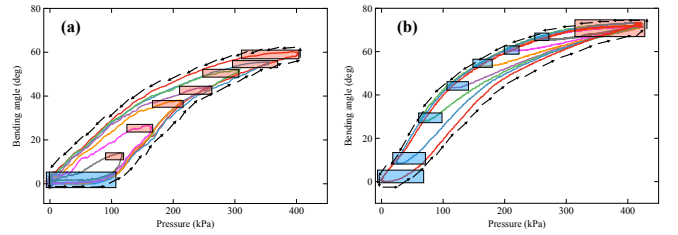


Fig. 5. Hysteresis loops: (a) results corresponding to the pressure variation in Fig 4 (a), (b): results that corresponds to (b) in the former Fig 4.

that have been extensively implemented for tasks with negligible time-related characteristics like controlling the longitudinal motion of simple PAM actuators [16], [22]. Additionally, the unique configuration of dual-PAM actuator introduces a high degree of freedom (DOF) into the control system, which significantly complicates the design and construction of model-based control algorithms or feedforward hysteresis compensators. Therefore, developing a simple yet effective control strategy is crucial for bend motion tracking using the dual-PAM actuator.

In this work, we deploy a control system composed of two separated subsystems with cascaded loops and *adaptforward* hysteresis compensators. By adhering to only fundamental guidelines, our system design reduces the effort required by engineers to address hysteresis affects in precisely controlling soft actuators with complex structure.

A. Design of Control System

The control system composes of two parallel subsystems. Each subsystem, structured in the cascade design with an outer loop and an inner loop, independently manages a single PAM of the actuator. This design can be visualized in Fig. 6, where black lines indicate forward paths from input reference value to output actual value, blue lines present the feedback paths, red and green lines exhibit the data transmission between a PID controller and the *adaptforward* hysteresis compensator. The outer loop is dedicated to position control that utilizes a PID controller. This inclusion is intended to counteract the intrinsic nonlinear dynamics characteristic of PAM operation, ensuring enhanced precision and response [15]. The inner loop is a pressure control loop involving another PID controller, responsible for the regulation and tracking of requisite

pressure to enable proficient position control. To account for the hysteresis, an *adaptforward* compensator is integrated into each subsystem. Alongside providing adjustments to the pressure reference value for the inner loop, this compensator also delivers adjustments to the PID controller in the outer position loop following the predicted variations of reference bending angle. Pressure reservoirs in the system play the role of storing and transferring pressure information. These reservoirs receive and store pressure adjustments from both PID controllers and hysteresis compensators, then publish the accumulated value as the reference pressure to the inner loop.

B. Design of Hysteresis Compensator

Fig. 7 is the schematic of the *adaptforward* hysteresis compensator, which consists of an adaptive program and a feedforward differential (D) controller that directly interfaces with the outer loop of subsystem. For boosting the generality of our design to not only pre-designed but also real-time references, low-pass filters are introduced for eliminating the effect brought by possibly existing sampling noise. Thus, the derivative values of reference are calculated through pseudo-differential operations as

$$\theta_d^{(i)}(t) = \frac{d}{dt} \left[\theta_d^{(i-1)}(t) \exp(-t/\tau) \right], (i = 1, 2, \dots), \quad (1)$$

where i is the order of pseudo-differential operation. The first and second order pseudo-differential values of the reference signal $\theta_d^{(1)}(t)$ and $\theta_d^{(2)}(t)$ are used respectively to indicate its velocities and accelerations in the following content. τ in both (1) and Fig. 7 is defined by $\tau = 1/(2\pi f_c)$, where f_c represents the low-pass cutoff frequency, which is set to 15 Hz in this work. The feedforward D gain K_{ff} is intended to compensate for the intrinsic response delay of the deformable soft actuator toward reference signal [23]. Its function is to process the first order pseudo-differential value of the desired bending angle $\theta_d^{(1)}(t)$ as expressed by

$$\Delta P_{ff} = K_{ff} \theta_d^{(1)}(t). \quad (2)$$

This calculated ΔP_{ff} is subsequently amalgamated with the pressure adjustment ΔP_{fb} from the outer loop PID controller, serving collectively as adjustment to the pressure reference for the inner loop.

Design of the feedforward factor is distinctly beneficial under conditions where the desired bending undergoes considerable variation with a correspondingly high differential value. Contrarily, the adaptive program is expected to operate when the desired bending changes slightly, where the feedforward component exerts limited effort due to low differential values. The adaptive program receives the reference signal with its first and second pseudo-differential values, then processes the input data and issues adjustments to the PID controller housed in the outer position loop, dynamically modifying its proportional gain.

In an effort to streamline the tuning process of PID gains, we instituted a regimen where the variations in internal pressures within the antagonistic PAMs were designed to mirror each other inversely. Thus, PID gains in the outer loops of two subsystems and the feedforward differential elements

in two hysteresis compensators are set to be opposite in sign. Meanwhile, parameter settings of the adaptive program, which will be detailed in the next subsection, are designed to be the same in different subsystems. Further, we set identical PID gains for inner loops in different subsystems to ensure uniform performance in pressure control for both PAMs.

C. Adaptive Law of Proportional Gain

Prior to delving into the adaptive rule in Fig. 7, it's crucial to establish several salient facts concerning bending tracking control using pneumatic soft actuators. (1) The tracking delay inherent in fluid-powered actuators, mainly instigated by hysteresis, tends to manifest predominantly during the transition between pressurization and depressurization states. This transition typically corresponds to U-turn motions in the target signal where the velocity direction changes. (2) Given that every exiting tracked target moves continuously, any directional alteration in its velocity is inevitably accompanied by deceleration-zero-acceleration progresses in the variation of target bending. (3) During the absence of rapid shifts in the tracked target's position, the reference signal can be seem as in quasi-static state, thus conventional PID controllers' performance can be improved by increasing the proportional gain to minimize the steady-state error and speed up the response [24]. However, an excessive increase in the proportional gain may lead to system instability when large scale changes occur in the reference as dynamic motion tracking control typically has more strict requirements for amplitude margin [25]. (4) Since hysteresis is invariant with respect to change rates of the input (internal pressures in this work) [26], one feasible method of alleviating the influence brought by hysteresis is to change the control signal so drastically that the system doesn't have enough time to react within the dead zones or quasi-dead zones and instead jumps over them.

The adaptive program uses the desired trajectory's motion pattern relating velocity and acceleration to predict its variation and adjust the dynamic proportional gain. Given the complexity of the nonlinear control system, capturing an exact one-to-one relationship between the dynamic PID gain and the reference signal is of limited feasibility. Additionally, if an exact linear relationship were adopted, environmental sampling noise in the reference signal and its differential values could cause significant oscillations in the dynamic gain. Therefore, we propose the adaptive law based on an accumulative operation. Firstly, if the acceleration of the desired bending angle $\theta_d^{(2)}(t)$ is negative, the adjustment in the dynamic proportional gain $\Delta K_P(t)$ is defined as:

$$\Delta K_P(t) = M_1 \frac{\theta_d(t)}{a_1} \frac{b_1}{b_1 + |\theta_d^{(1)}(t)|} \frac{|\theta_d^{(2)}(t)|}{c_1 + |\theta_d^{(2)}(t)|} D(t). \quad (3)$$

Conversely, for any positive $\theta_d^{(2)}(t)$ values, the adjustment $\Delta K_P(t)$ is determined by

$$\Delta K_P(t) = M_2 \frac{\Theta - \theta_d(t)}{a_2} \frac{b_2}{b_2 + |\theta_d^{(1)}(t)|} \frac{|\theta_d^{(2)}(t)|}{c_2 + |\theta_d^{(2)}(t)|} D(t). \quad (4)$$

Naturally, $\Delta K_P(t)$ is set to 0 by any other circumstances.

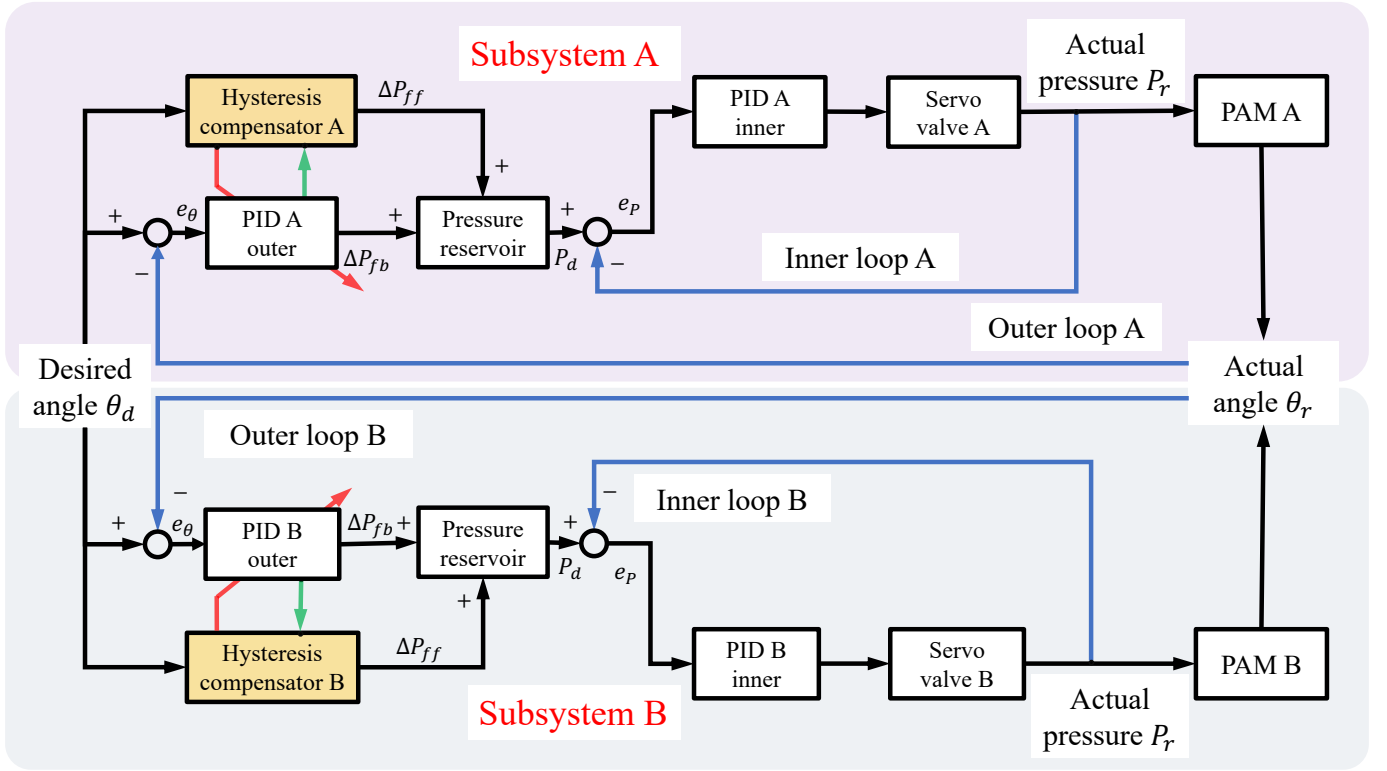


Fig. 6. Configuration of the control system with two subsystems respectively manipulating two independent PAMs.

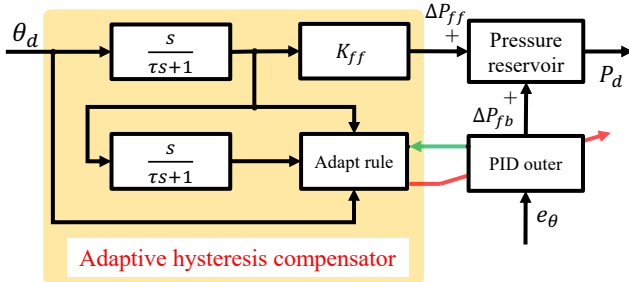


Fig. 7. Structure of the *adaptforward* hysteresis compensator.

In the preceding definitions, $\theta_{\text{ref}}(t)$ signifies the reference bending angle, Θ represents its predetermined variation range, and $K_P(0)$ denotes the initial proportional gain of the PID controller. a is employed to simulate the correlation between the width of dead-zones or quasi-dead-zones and reference bending angle, as observed in the hysteresis loops in Fig. 5. b is used to ensure the proportional gain varying smoothly, restricting the gain's augmentation when the tracked bending motion is in drastic changing, while allowing the gain to increase rapidly as the reference's change slows down. The change in b influences both the smoothness of the overall gain variations and the disparity between the change rates of gain during periods of fast and slow reference changing. c is the acceleration coefficient that ensures an adjustable amplification in the dynamic gain consistent with the angular acceleration of the reference bending. Implementation of c prevents an excessive increase in the proportional gain

during slow reference angular velocity changes and ensures a sufficient increase by a short period when the reference's angular velocity varies rapidly. By changing the values of a , b , and c , the system can show either enhanced stability with more conservative performance toward hysteresis or higher hysteresis resistance but more vulnerability to disturbance occurring during the reference bending's U-turn changes. $D(t)$, as defined by

$$D(t) = - \left(1 + \frac{1+h(t)}{2} \cdot \mu \right) h(t), \quad (5)$$

functions as a direction changer. $h(t)$ here is a sign function as

$$h(t) = \text{sign}(\theta_d^{(1)}(t)\theta_d^{(2)}(t)). \quad (6)$$

The directional term either augments or reduces the proportional gain in alignment with variations in motion states of the desired bending angle. μ in (6) is imposed as an augment operator used to apply a natural decrease tendency to the dynamic proportional gain for the consideration of maintaining system stability from sustained high gain values. Simultaneously, for maintaining a baseline value of the dynamic proportional gain as $K_P(0)$, a cutoff operation represented by

$$K_P(t) = \max\{K_P(0), K_P(t-1) + \Delta K_P(t)\} \quad (7)$$

is implemented with each update. Lastly, M is introduced for ensuring a formally dimensional consistency on both sides of the equation. Paring down parameters, (3) can be restructured

TABLE I
PID GAINS IN SUBSYSTEM A.

Gain	Value	Unit
Inner - P	4.0×10^{-2}	V/kPa
Inner - I	2.0×10^{-6}	V/kPa · s
Inner - D	0	V · s/kPa
Outer - P	8.0×10^{-2}	kPa/deg
Outer - I	2.0×10^{-5}	kPa/deg · s
Outer - D	0	kPa · s/deg
Feedforward - D	1.0×10^{-2}	kPa · s/deg

as

$$\Delta K_P(t) = M_1^* \frac{\theta_d(t)|\theta_d^{(2)}(t)|}{(b_1 + |\theta_d^{(1)}(t)|)(c_1 + |\theta_d^{(2)}(t)|)} D(t), \quad (8)$$

while (4) can be articulated as

$$\Delta K_P(t) = M_2^* \frac{(\Theta - \theta_d(t))|\theta_d^{(2)}(t)|}{(b_2 + |\theta_d^{(1)}(t)|)(c_2 + |\theta_d^{(2)}(t)|)} D(t). \quad (9)$$

IV. EXPERIMENTAL VALIDATION

Experimental studies validate the effectiveness of our novel control method, demonstrating its practical utility in bending trajectory tracking with the dual-PAM soft actuator. Comparative tests across diverse reference signals are employed to provide comprehensive evaluations on the performance of the newly proposed *adaptforward* control over traditional options.

A. Experimental Setup

The reference signals are modeled as three distinct types of waves; the first type is a sinusoidal wave progressively increases in amplitude with a constant frequency, the second type is a sinusoidal wave maintains a constant amplitude while steadily increasing its frequency, and the third reference signal is a compound waveform. These signals are applied periodically and repeatedly during each experiment. For our experiments, a 500 Hz sampling frequency is set for the reference the actual bending angle, the pressures of the PAMs, and the frequency of proportional gain updating. Through a trial-and-error method, we ascertained parameters in the *adaptforward* control system: gains for PID controllers in cascade loops, gains for the feedforward D gain in the hysteresis compensator, and all factors used in the adaptive program. These identified parameters are provided in Tables I and II. To save space, only PID gains in subsystem A are demonstrated in Table I, gain values used in subsystem B can be deduced following the description in the former *Design of Hysteresis Compensator* section. Our experimental evaluation compares the performance of three different control schemes: traditional PID, PID with the feedforward differential element in the hysteresis compensator, and PID with both feedforward element and adaptive rule in the compensator.

B. Experimental Results and Discussion

In the context of the first reference signal, as depicted in Fig. 8, the performance of the traditional PID controller

TABLE II
PARAMETERS IN ADAPTIVE RULE.

Parameter	Value	Unit
M_1^*	6.0×10^{-2}	kPa/deg · s
b_1	6.0	deg/s
c_1	3.2×10^4	deg/s ²
M_2^*	9.6×10^{-2}	kPa/deg · s
b_2	6.0	deg/s
c_2	5.0×10^4	deg/s ²
Θ	60	deg
μ	0.6	/

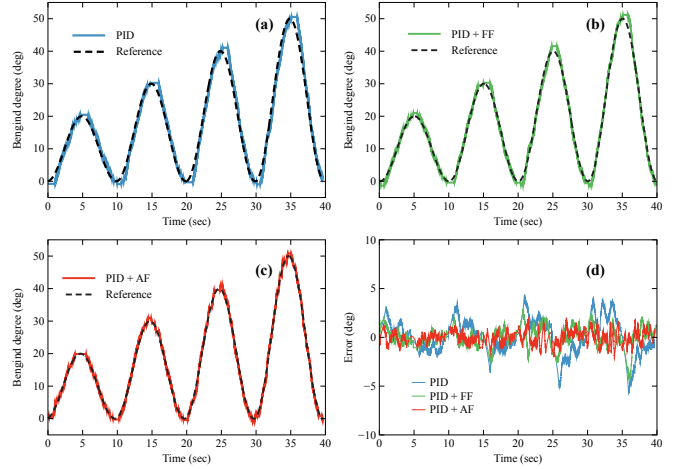


Fig. 8. Experimental results with the first waveform: (a) PID (blue), (b) PID with the feedforward differential element (green), (c) the proposed *adaptforward* control (red), and (d) tracking errors associated with different control strategies.

exhibits degeneration as the variation range of the desired bending broadens, particularly at moments where the velocity direction undergoes reversal. While the integration of the feedforward differential gain effectively mitigates the range and peak value of the tracking error, its performance invariably deteriorates with the expansion of reference signal's variation range. This deterioration is evidenced by a discernible delay in response to the reversal of the reference bending's direction. In contrast, the *adaptforward* control markedly diminishes the tracking error across the entire variation range. Numerical results indicate a reduction in the maximal tracking error from 5.68 degrees, as seen with the traditional PID controller, to 4.35 degrees when feedforward differential component being applied, and the employment of *adaptforward* hysteresis compensator further reduces it to 1.97 degrees.

Fig. 9 depicts the results obtained using the second reference signal. Analogous to the previous scenario, the control performance of different controllers mildly degrades with an increase in the reference trajectory's frequency, resulting in pronounced tracking errors, especially at higher frequencies. The conventional PID controller in isolation exhibits a palpable deviation owing to its inadequate handling of the delay engendered by hysteresis. Although the integration of feedforward differential component mitigates this deviation to some

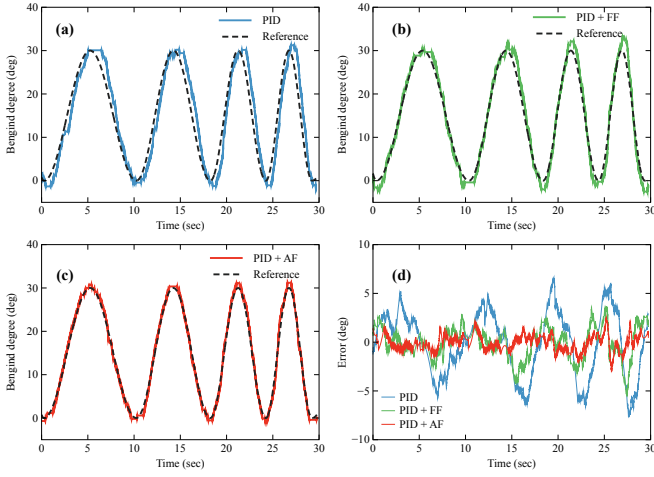


Fig. 9. Experimental results with the second waveform: (a) PID (blue), (b) PID with the feedforward differential element (green), (c) the proposed *adaptforward* control (red), and (d) tracking errors.

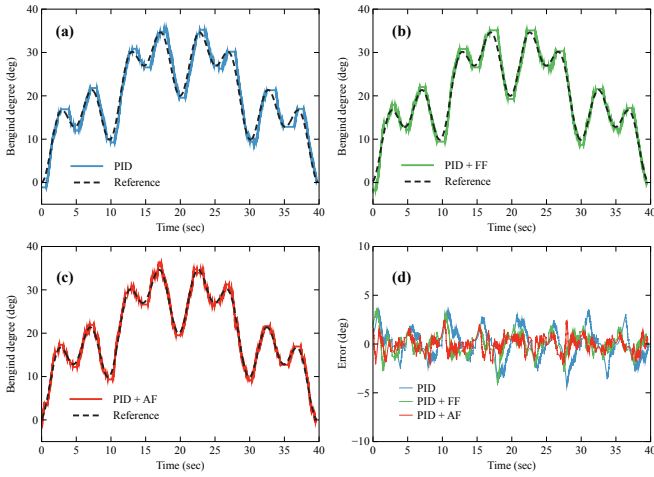


Fig. 10. Experimental results with the third waveform: (a) PID (blue), (b) PID with the feedforward differential element (green), (c) the proposed *adaptforward* control (red), and (d) tracking errors.

extent, its performance wanes as the frequency continues escalating. The *adaptforward* hysteresis compensator, on the other hand, enhances the system's tracking performance across a range of low frequencies, and maintains close adherence to the target trajectory even at high frequencies.

Fig. 10 showcases the results with the third complex reference signal. Utilizing the conventional PID controller results in conspicuous tracking errors, particularly at points where the desired trajectory alters direction, irrespective of the magnitude of the reference trajectory's maneuver. The inclusion of feedforward differential component alleviates such errors during maneuvers of lesser magnitude in the reference trajectory. However, tracking errors become evident as the maneuver acquires a relatively large magnitude. Meanwhile, the proposed *adaptforward* control rectifies most tracking errors during both minor and drastic motion alterations. Herein, a better performance of the *adaptforward* control in tracking complex trajectories is proved.

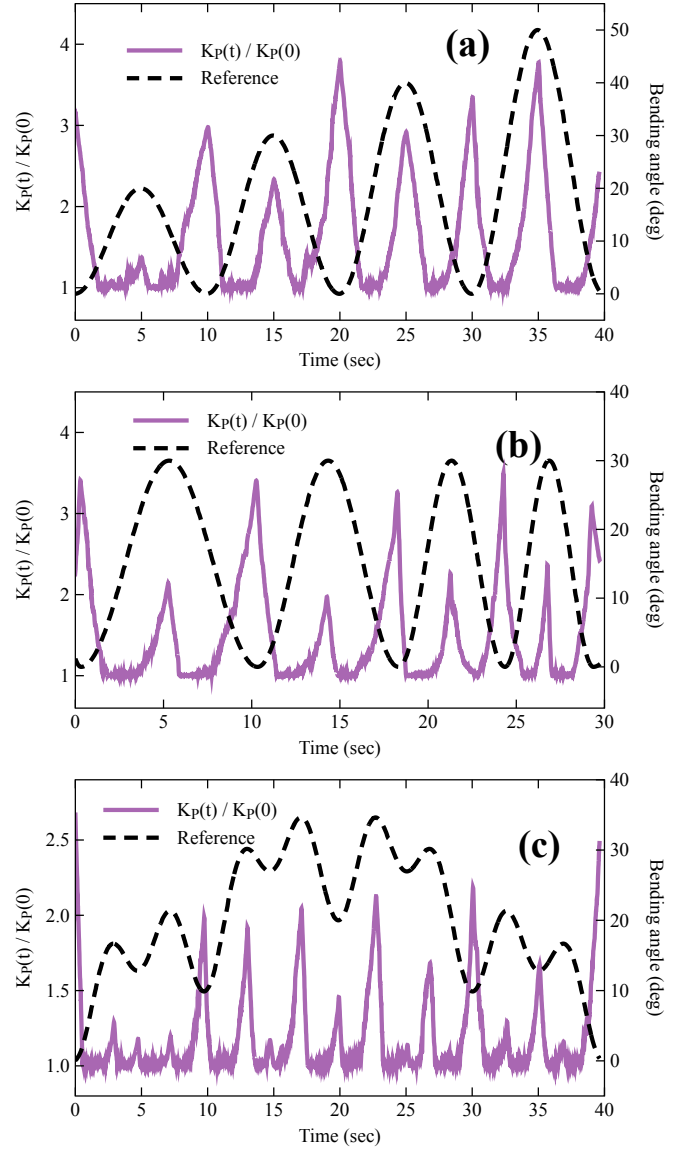


Fig. 11. Amplification ratio of proportional gain correspond to different references: (a) the first sinusoidal waveform, (b) the second sinusoidal waveform, and (c) a compound waveform.

Fig. 11 depicts the amplification ratio of the PID controller's proportional gain, where $K_P(t)$ and $K_P(0)$ respectively represent the current value and initial value of the dynamic proportional gain. With the imposed naturally decreasing tendency, the amplification ratio swiftly reverts to a low value as the reference bending trajectory withdraws from direction reversing zones. During rapid varying periods of the desired signal, the amplification ratio maintains a steadily low value of 1. Concurrently, observable increases and peaks coincide with locations where the reference trajectory decelerates to change its direction. This dynamic demonstrates the adaptability and resiliency of the adaptive program under different bending motion trackings.

V. CONCLUSION

We achieved precise trajectory tracking control using a dual-PAM bending actuator and a hysteresis compensation scheme. The bending actuator features two independently controlled PAMs separated by a central metal plate. This configuration imparts enhanced and potentially adjustable rigidity to the overall structure, whilst the antagonistic arrangement and inherent elasticity of the metal facilitates a swift response. The hysteresis characteristics of this pneumatic actuator were investigated through experiments, revealing the correlation between widths of hysteresis dead-zones and quasi dead-zones and the bending angle.

To facilitate an accurately controllable bending, we introduced a control system integrating two cascaded PID loops with newly proposed *adaptforward* hysteresis compensators. The *adaptforward* compensator is a unique design combining an adaptive program and a feedforward differential controller. Based on the predicted variations of the reference bending trajectory, the adaptive program enables dynamic adjustments in the proportional gain of the PID controller within the outer cascade loop. The proposed control method to reduce hysteresis-induced tracking errors has been experimentally validated using a variety of reference signals, demonstrating its versatility and efficiency. This control method is simple yet effective for actuators exhibiting hysteresis, consequently expanding the range of potential applications for soft actuators in the fields of robotics and automation.

REFERENCES

- [1] D. Rus and M. T. Tolley, "Design, fabrication and control of soft robots," *Nature*, vol. 521, no. 7553, pp. 467–475, 2015.
- [2] O. Azami, D. Morisaki, T. Miyazaki, T. Kanno, and K. Kawashima, "Development of the extension type pneumatic soft actuator with built-in displacement sensor," *Sensors and Actuators A: Physical*, vol. 300, p. 111623, 2019. [Online]. Available: <https://www.sciencedirect.com/science/article/pii/S0924424719307538>
- [3] X. Huang, K. Kumar, M. K. Jawed, A. M. Nasab, Z. Ye, W. Shan, and C. Majidi, "Chasing biomimetic locomotion speeds: Creating untethered soft robots with shape memory alloy actuators," *Science Robotics*, vol. 3, no. 25, p. eaau7557, 2018.
- [4] R. Hisatomi, T. Kanno, T. Miyazaki, T. Kawase, and K. Kawashima, "Development of forceps manipulator using pneumatic soft actuator for a bending joint of forceps tip," in *2019 IEEE/SICE International Symposium on System Integration (SII)*, 2019, pp. 695–700.
- [5] T. Miyazaki, T. Tagami, D. Morisaki, R. Miyazaki, T. Kawase, T. Kanno, and K. Kawashima, "A motion control of soft gait assistive suit by gait phase detection using pressure information," *Applied Sciences*, vol. 9, no. 14, 2019. [Online]. Available: <https://www.mdpi.com/2076-3417/9/14/2869>
- [6] H. Lipson, "Challenges and opportunities for design, simulation, and fabrication of soft robots," *Soft Robotics*, vol. 1, no. 1, pp. 21–27, 2014. [Online]. Available: <https://doi.org/10.1089/soro.2013.0007>
- [7] H. Aschemann and D. Schindele, "Comparison of model-based approaches to the compensation of hysteresis in the force characteristic of pneumatic muscles," *IEEE Transactions on Industrial Electronics*, vol. 61, no. 7, pp. 3620–3629, 2013.
- [8] T. Helps and J. Rossiter, "Proprioceptive flexible fluidic actuators using conductive working fluids," *Soft robotics*, vol. 5, no. 2, pp. 175–189, 2018.
- [9] H. Zhao, Y. Li, A. Elsamadisi, and R. Shepherd, "Scalable manufacturing of high force wearable soft actuators," *Extreme Mechanics Letters*, vol. 3, pp. 89–104, 2015.
- [10] C. Laschi and M. Cianchetti, "Soft robotics: new perspectives for robot bodyware and control," *Frontiers in bioengineering and biotechnology*, vol. 2, p. 3, 2014.
- [11] G. Endo and N. Otomo, "Development of a food handling gripper considering an appetizing presentation," in *2016 IEEE International Conference on Robotics and Automation (ICRA)*, 2016, pp. 4901–4906.
- [12] W. M. KIER and K. K. SMITH, "Tongues, tentacles and trunks: the biomechanics of movement in muscular-hydrostats," *Zoological Journal of the Linnean Society*, vol. 83, no. 4, pp. 307–324, 06 2008. [Online]. Available: <https://doi.org/10.1111/j.1096-3642.1985.tb01178.x>
- [13] X. Zang, Y. Liu, S. Heng, Z. Lin, and J. Zhao, "Position control of a single pneumatic artificial muscle with hysteresis compensation based on modified prandtl-ishlinskii model," *Bio-Medical Materials and Engineering*, vol. 28, no. 2, pp. 131–140, 2017.
- [14] F. Schreiber, Y. Sklyarenko, K. Schlüter, J. Schmitt, S. Rost, A. Raatz, and W. Schumacher, "Tracking control with hysteresis compensation for manipulator segments driven by pneumatic artificial muscles," in *2011 IEEE international conference on robotics and biomimetics*. IEEE, 2011, pp. 2750–2755.
- [15] S. Xie, J. Mei, H. Liu, and Y. Wang, "Hysteresis modeling and trajectory tracking control of the pneumatic muscle actuator using modified prandtl-ishlinskii model," *Mechanism and Machine Theory*, vol. 120, pp. 213–224, 2018.
- [16] G. Shi and W. Shen, "Hybrid control of a parallel platform based on pneumatic artificial muscles combining sliding mode controller and adaptive fuzzy cmac," *Control Engineering Practice*, vol. 21, no. 1, pp. 76–86, 2013. [Online]. Available: <https://www.sciencedirect.com/science/article/pii/S0967066112001931>
- [17] X. Zhao and Y. Tan, "Neural network based identification of preisach-type hysteresis in piezoelectric actuator using hysteretic operator," *Sensors and Actuators A: Physical*, vol. 126, no. 2, pp. 306–311, 2006.
- [18] H. Aschemann and D. Schindele, "Comparison of model-based approaches to the compensation of hysteresis in the force characteristic of pneumatic muscles," *IEEE Transactions on Industrial Electronics*, vol. 61, no. 7, pp. 3620–3629, 2014.
- [19] X. Zhu, G. Tao, B. Yao, and J. Cao, "Adaptive robust posture control of a parallel manipulator driven by pneumatic muscles," *Automatica*, vol. 44, no. 9, pp. 2248–2257, 2008. [Online]. Available: <https://www.sciencedirect.com/science/article/pii/S0005109808000654>
- [20] S. Xie, G. Ren, J. Xiong, and Y. Lu, "A trajectory tracking control of a robot actuated with pneumatic artificial muscles based on hysteresis compensation," *IEEE Access*, vol. 8, pp. 80 964–80 977, 2020.
- [21] C.-P. Chou and B. Hannaford, "Measurement and modeling of mckibben pneumatic artificial muscles," *IEEE Transactions on robotics and automation*, vol. 12, no. 1, pp. 90–102, 1996.
- [22] M.-D. Duong, Q.-T. Pham, T.-C. Vu, N.-T. BUI, and D. Thinh, "Adaptive fuzzy sliding mode control of an actuator powered by two opposing pneumatic artificial muscles," *Scientific Reports*, vol. 13, 05 2023.
- [23] J. Chen, S. Fang, and H. Ishii, "Fundamental limitations and intrinsic limits of feedback: An overview in an information age," *Annual Reviews in Control*, vol. 47, pp. 155–177, 2019.
- [24] H. Li, W. Liu, K. Wang, K. Kawashima, and E. Magid, "A cable-pulley transmission mechanism for surgical robot with backdrivable capability," *Robotics and Computer-Integrated Manufacturing*, vol. 49, pp. 328–334, 2018. [Online]. Available: <https://www.sciencedirect.com/science/article/pii/S0736584516302356>
- [25] K. H. Ang, G. Chong, and Y. Li, "Pid control system analysis, design, and technology," *IEEE transactions on control systems technology*, vol. 13, no. 4, pp. 559–576, 2005.
- [26] A. Visintin, *Differential models of hysteresis*. Springer Science & Business Media, 2013, vol. 111.